The Understanding of Pollutant Transport in the Atmosphere: Lagrangian Coherent Structures

Peter Nolan, Hosein Foroutan, Shane Ross

Department of Biomedical Engineering and Mechanics, Virginia Tech, Blacksburg VA, USA

contact email: foroutan@vt.edu

Introduction

Eulerian chemical transport models (e.g., CMAQ) are powerful tools to simulate the transport and fate of air pollutants in various scales from local to global. Informed by meteorological drivers (e.g., WRF), these models calculate the advection of gases and aerosols in the atmosphere and provide information about how pollutants are transported from one location to another.

Identifying atmospheric transport pathways and barriers is important to understand pollutants effects on weather, climate, and human health. The atmospheric wind field is variable in space and time and contains complex patterns due to turbulence mixing. In such a highly unsteady flow field, streamlines (Eulerian entities showing the local direction of the velocity at any given instant) do not provide useful information regarding the transport over a finite time. Therefore, particle trajectories are often used to study how pollutants move in the atmosphere. Nevertheless, individual trajectories are sensitive to their initial conditions, cannot fully resolve the complexity of the flow, and often result in a chaotic and tangled field difficult to analyze. Therefore, a more systematic and robust approach is needed.

Lagrangian Coherent Structures (LCS)

Lagrangian Coherent Structures (LCS) form the template of fluid particle motion in a fluid flow. LCS can be characterized by special material surfaces that organize the particle motion into ordered patterns. They are classified as hyperbolic attracting, hyperbolic repelling, parabolic, and elliptical. These key material surfaces form the core of fluid deformation patterns, such as saddle points, tangles, filaments, and pathways.

LCS can be diagnosed using the finite-time Lyapunov exponent (FTLE). The FTLE gives a measure of material stretching in fluid flows. It arises from the dynamical system,

$$\frac{d\boldsymbol{x}}{dt} = \boldsymbol{v}(\boldsymbol{x},t),$$
$$\boldsymbol{x}_0 = \boldsymbol{x}(t_0),$$

and is defined as

$$\sigma_{t_0}^{t_f}(\boldsymbol{x}) = \frac{1}{2|t_f - t_0|}\log\left(\lambda_{t_0}^{t_f}(\boldsymbol{x})\right),$$

where $\boldsymbol{v}(\boldsymbol{x},t)$ is a general velocity field and $\lambda_{t_0}^{t_f}$ is the largest eigenvalue of the Cauchy-Green strain tensor over the period from t_0 to t_f. Hyperbolic attracting structures coincide with ridges of the backward-time FTLE field, hyperbolic repelling structures coincide with ridges of the forward-time FTLE field, parabolic structures tend to coincide with troughs of the FTLE field, and elliptical structures tend to be bordered by ridges in both the forward-time and backward-time FTLE fields.

LCS is emerging as an important tool for evaluating fluid transport in engineering, medicine, environmental, and geophysical settings. They have been demonstrated to be predictive for both mesoscale oceanic and atmospheric fluid flows.

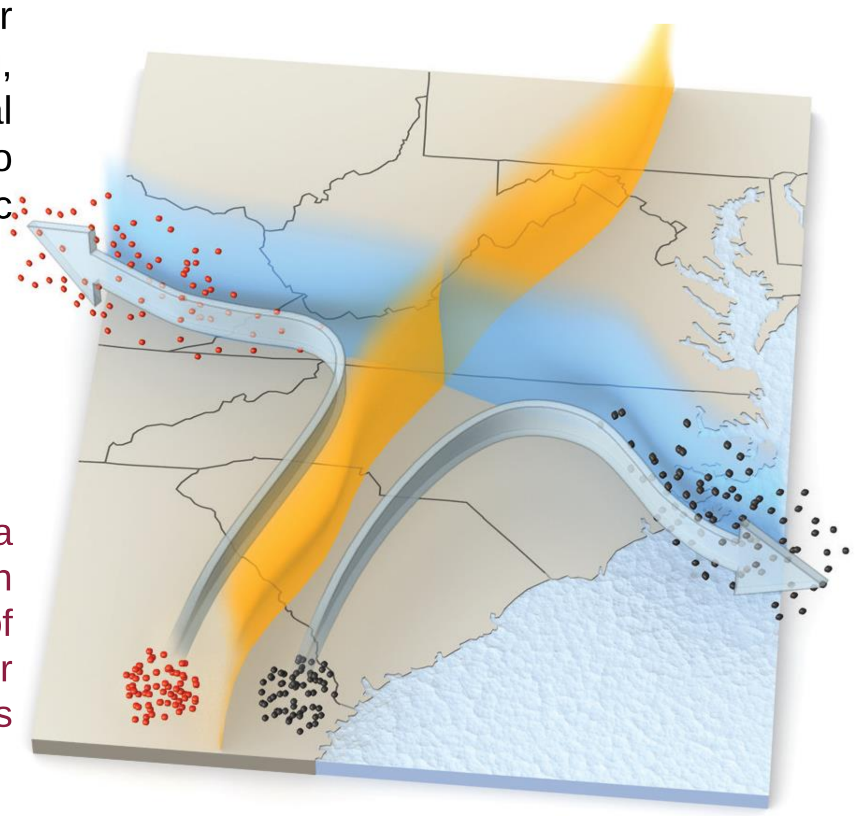

Schematic of an attracting LCS (blue), a repelling LCS (orange), and their intersection known as a saddle point. Two groups of particles that start fairly close to each other travel hundreds of miles in opposite directions once they hit the center of the saddle point.

Regional LCS: CMAQ Simulations

Analyses are based on CMAQ v5.2 benchmark test case of Southeast United States.

- CMAQ v5.2
- 12-km uniform horizontal grid
- 35 vertical layers expanding up to 50 hPa
- 24-hr simulations started at July 1, 2011, 00:00:00 UTC

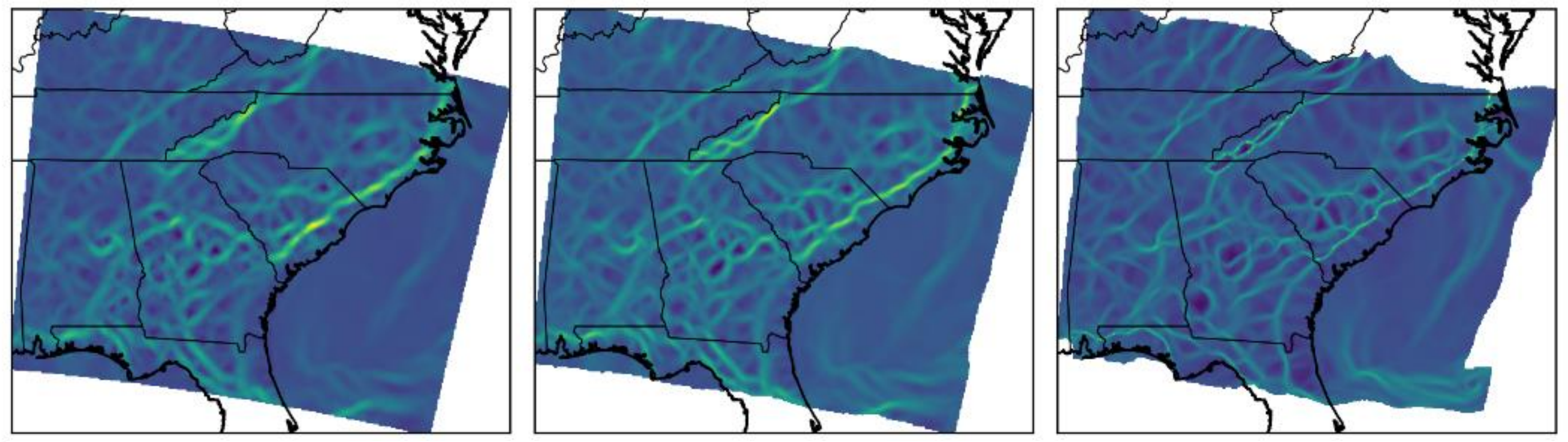

Backward FTLE fields for 21:00 UTC, July 1 2011 calculated based on horizontal wind vector components at 80-m height. Integration time is 0 hr (left), -1 hr (center), and -6 hr (right). High FTLE values (attracting regions) are shown in yellow.

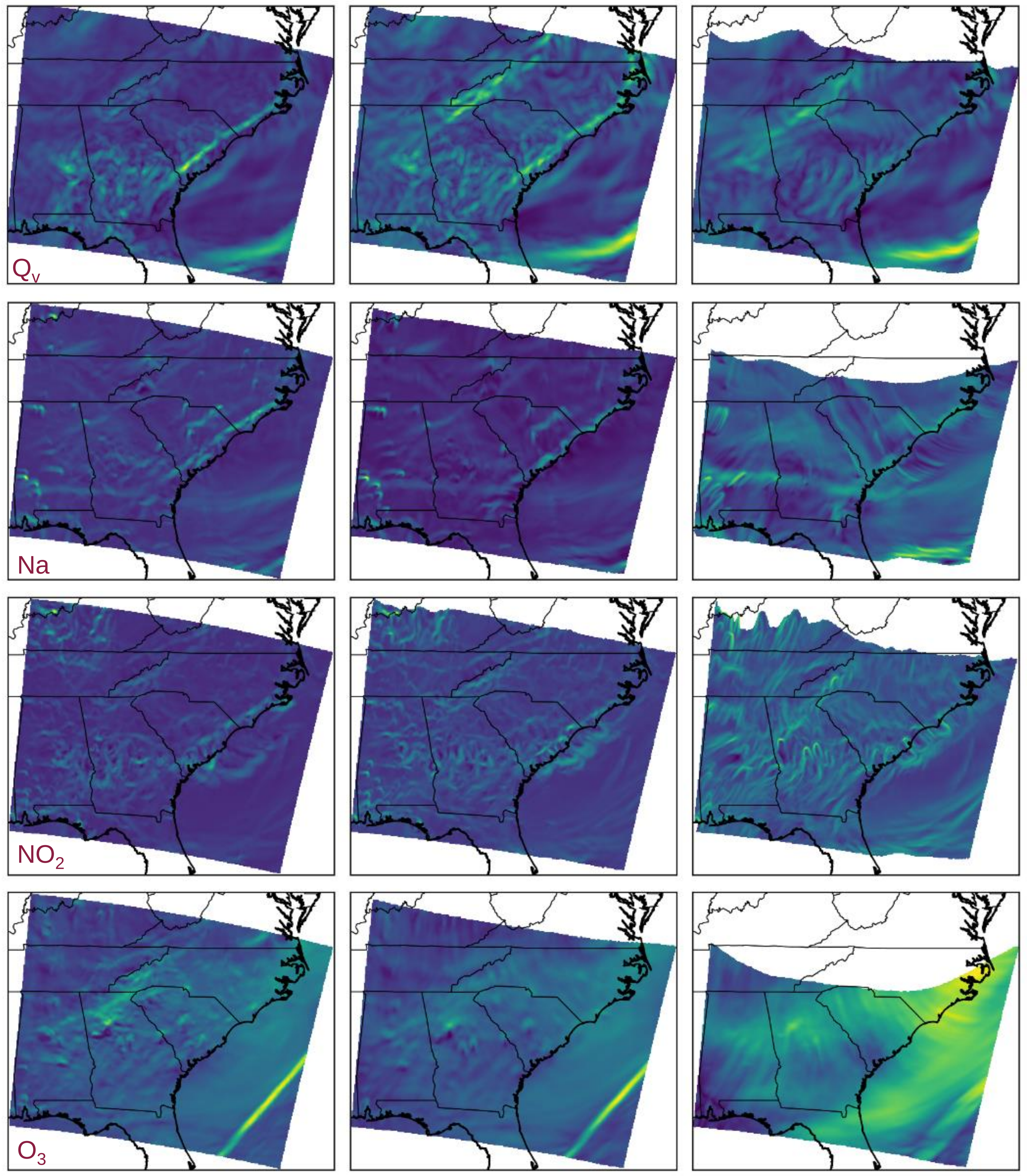

Backward FTLE fields for 21:00 UTC, July 1 2011 calculated based on column-averaged and species-weighted horizontal wind vector components:

$$\boldsymbol{v}(\boldsymbol{x},t) = \begin{cases} \int_0^1 uq\frac{\partial p}{\partial \eta}d\eta \,/ \int_0^1 q\frac{\partial p}{\partial \eta}d\eta \\ \int_0^1 vq\frac{\partial p}{\partial \eta}d\eta \,/ \int_0^1 q\frac{\partial p}{\partial \eta}d\eta \end{cases}$$

Integration time is 0 hr (left), -1 hr (center), and -6 hr (right). High FTLE values (attracting regions) are shown in yellow.

Global LCS: MPAS-A Simulations

Simulations are performed using Model for Prediction Across Scales-Atmosphere (MPAS-A), a global fully compressible non-hydrostatic model with centroidal Voronoi grids (nominally hexagonal).

- MPAS-A v5.1
- 120-km and 60-km uniform horizontal mesh
- 41 vertical layers expanding up to 22 km
- “Mesoscale_reference” physics suite, including YSU planetary boundary layer, RRTMG SW and LW radiation, new Tiedtke convection, WSM6 microphysics, and Noah land surface models.
- 24-hr simulations started at September 28, 2010, 12:00:00 UTC

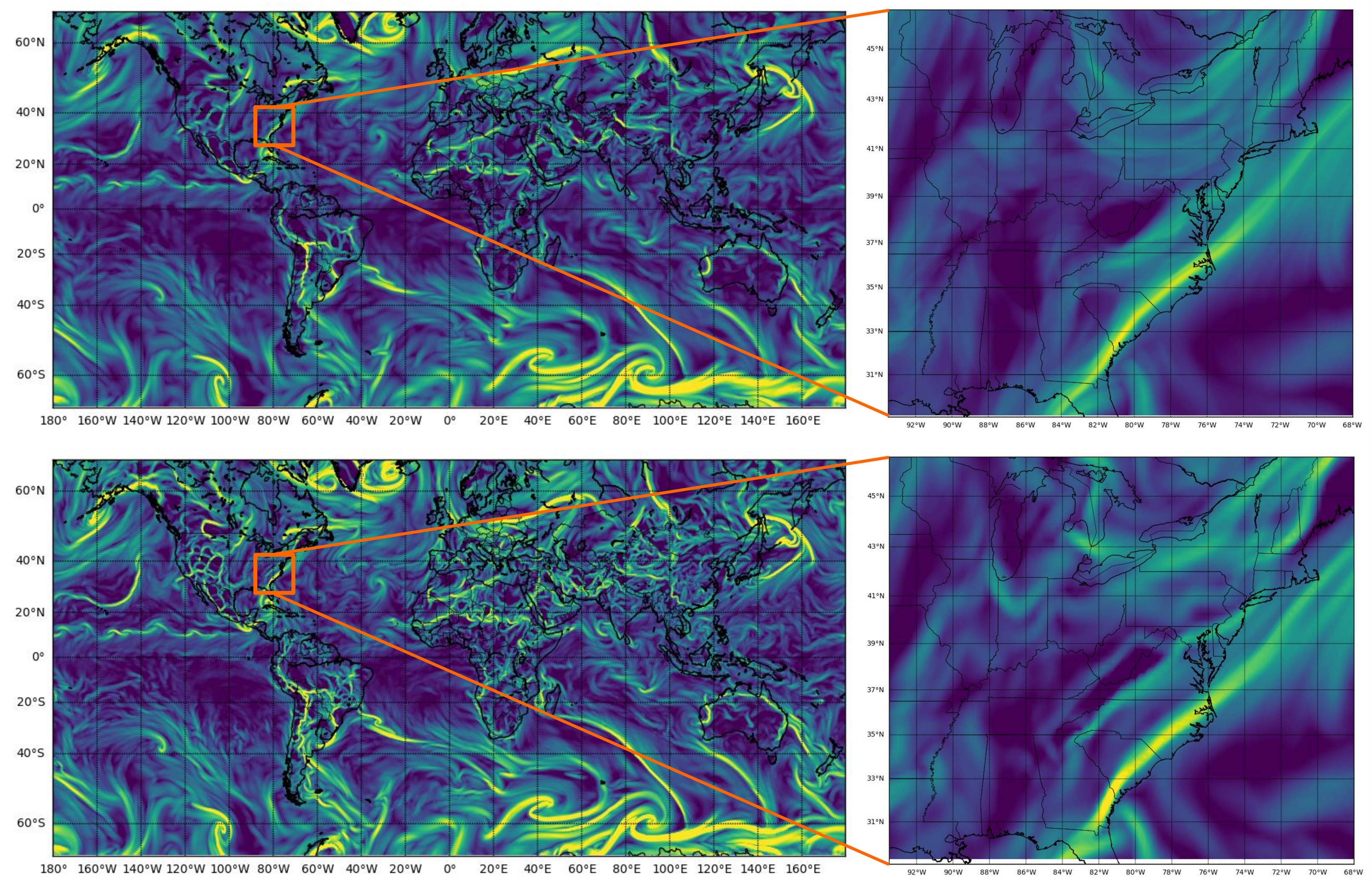

Backward FTLE fields for 12:00 UTC, Sep 29 2010 calculated based on horizontal wind vector components at 850 hPa height on a 120-km mesh (top) and 60-km mesh (bottom). Integration time is -24 hr. High FTLE values (attracting regions) are shown in yellow.

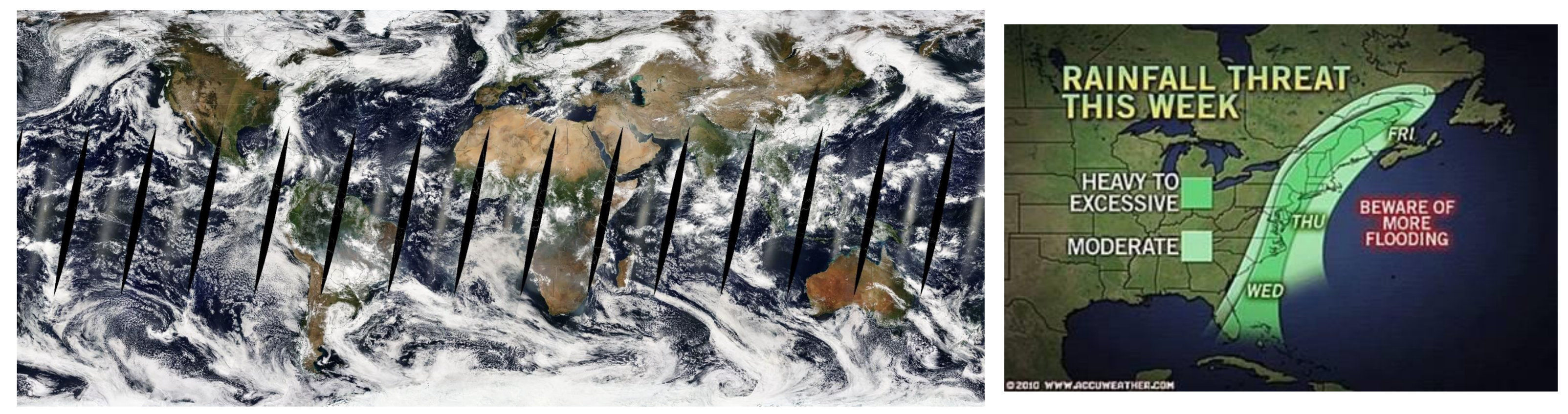

MODIS Terra corrected reflectance (true color) for Sep 29 2010 (left), and a weather alert about an extremely heavy rain in the East Coast of the United States on the same day (right).

Ongoing and Future Research

- Extend the analysis to various vertical layers and 3-D LCS.
- Extend to other test cases over various temporal and spatial scales.
- Develop LCS based on field measurements and combine with data from simulations.
- Compare LCS fields with satellite and remote-sensing observations.
- Use LCS to improve reduced-order models.
- Study the implication of LCS (weighted by various species) to source locations, atmospheric chemistry, and exposure.

17th Annual CMAS Conference
October 22-24, 2018